Two-photon fluorescence correlation spectroscopy of lipid-encapsulated fluorescent nanodiamonds in living cells

Yuen Yung Hui,[1] Bailin Zhang,[1] Yuan-Chang Chang,[1] Cheng-Chun Chang,[1] Huan-Cheng Chang,[1,*] Jui-Hung Hsu,[2] Karen Chang,[3] and Fu-Hsiung Chang[4]

[1]Institute of Atomic and Molecular Sciences, Academia Sinica, Taipei 106, Taiwan, ROC
[2]Department of Materials and Optoelectronic Science, National Sun Yat-Sen University, Kaohsiung 804, Taiwan, ROC
[3]Graduate Institute of Oral Biology, National Taiwan University, Taipei 100, Taiwan, ROC
[4]Graduate Institute of Biochemistry and Molecular Biology, National Taiwan University, Taipei 100, Taiwan, ROC
**hcchang@po.iams.sinica.edu.tw*

Abstract: Dynamics of fluorescent diamond nanoparticles in HeLa cells has been studied with two-photon fluorescence correlation spectroscopy (FCS). Fluorescent nanodiamond (FND) is an excellent fluorescent probe for bioimaging application, but they are often trapped in endosomes after cellular uptake. The entrapment prohibits FCS from being performed in a time frame of 60 s. Herein, we show that the encapsulation of FNDs within a lipid layer enhances the diffusion of the particles in the cytoplasm by more than one order of magnitude, and particles as small as 40 nm can be probed individually with high image contrast by two-photon excited luminescence. The development of the technique together with single particle tracking through one-photon excitation allows probing of both short-term and long-term dynamics of single FNDs in living cells.

OCIS codes: (160.4236) Nanomaterials; (180.2520) Fluorescence microscopy; (300.6410) Spectroscopy, multiphoton; fluorescence correlation spectroscopy; fluorescent nanodiamond; liposome; single particle tracking; two-photon excitation.

References and links

1. K. M. Berland, P. T. C. So, and E. Gratton, "Two-photon fluorescence correlation spectroscopy: method and application to the intracellular environment," Biophys. J. **68**, 694-701 (1995).
2. P. Schwille, U. Haupts, S. Maiti, and W. W. Webb, "Molecular dynamics in living cells observed by fluorescence correlation spectroscopy with one- and two-photon excitation," Biophys. J. **77**, 2251-2265 (1999).
3. V. Levi and E. Gratton, "Exploring dynamics in living cells by tracking single particles," Cell Biochem. Biophys. **48**, 1-15 (2007).
4. D. R. Larson, W. R. Zipfel, R. M. Williams, S. W. Clark, M. P. Bruchez, F. W. Wise, and W. W. Webb, "Water-soluble quantum dots for multiphoton fluorescence imaging in vivo," Sci. **300**, 1434-1436 (2003).
5. H. Wang, T. B. Huff, D. A. Zweifel, W. He, P. S. Low, A. Wei, and J.-X. Cheng, "In vitro and in vivo two-photon luminescence imaging of single gold nanorods," Proc. Natl. Acad. Sci. USA **102**, 15752-15756 (2005).
6. W. H. Pohl, H. Hellmuth, M. Hilbert, J. Seibel, and P. J. Walla, "A two-photon fluorescence-correlation study of lectins interacting with carbohydrated 20 nm beads," ChemBioChem **7**, 268-274 (2006).
7. C.-S. Chen, J. Yao, and R. A. Durst, "Liposome encapsulation of fluorescent nanoparticles: Quantum dots and silica nanoparticles," J. Nanoparticle Res. **8**, 1033-1038 (2006).
8. R. F. Heuff, J. L. Swift, and D. T. Cramb, "Fluorescence correlation spectroscopy using quantum dots: advances, challenges and opportunities," Phys. Chem. Chem. Phys. **9**, 1870-1880 (2007).
9. P. Didier, G. Ulrich, Y. Mély, and R. Ziessel, "Improved push-pull-push E-Bodipy fluorophores for two-photon cell-imaging," Org. Biomol. Chem. **7**, 3639-3642 (2009).
10. Z. Petrasek, C. Hoege, A. Mashaghi, T. Ohrt, A. A. Hyman, and P. Schwille, "Characterization of protein dynamics in asymmetric cell division by scanning fluorescence correlation spectroscopy," Biophys. J. **95**, 5476-5486 (2008).
11. R. Briandet, P. Lacroix-Gueu, M. Renault, S. Lecart, T. Meylheuc, E. Bidnenko, K. Steenkeste, M.-N. Bellon-Fontaine, and M.-P. Fontaine-Aupar, "Fluorescence correlation spectroscopy to study diffusion and reaction of bacteriophages inside biofilms," Appl. Environ. Microbiol. **74**, 2135-2143 (2008).

#120224 - $15.00 USD Received 19 Nov 2009; revised 6 Jan 2010; accepted 7 Jan 2010; published 10 Mar 2010

12. Q. Ruan, Y. Chen, E. Gratton, M. Glaser, and W. W. Mantulin, "Cellular characterization of adenylate kinase and its isoform: Two-photon excitation fluorescence imaging and fluorescence correlation spectroscopy," Biophys. J. **83**, 3177-3187 (2002).
13. S.-J. Yu, M.-W. Kang, H.-C. Chang, K.-M. Chen, and Y.-C. Yu, "Bright fluorescent nanodiamonds: No photobleaching and low cytotoxicity," J. Am. Chem. Soc. **127**, 17604-17605 (2005).
14. C.-C. Fu, H.-Y. Lee, K. Chen, T.-S. Lim, H.-Y. Wu, P.-K. Lin, P.-K. Wei, P.-H. Tsao, H.-C. Chang, and W. Fann, "Characterization and application of single fluorescent nanodiamonds as cellular biomarkers," Proc. Natl. Acad. Sci. USA **104**, 727-732 (2007).
15. F. Neugart, A. Zappe, F. Jelezko, C. Tietz, J.-P. Boudou, A. Krueger, and J. Wrachtrup, "Dynamics of diamond nanoparticles in solution and cells," Nano Lett. **7**, 3588-3591 (2007).
16. Y.-R. Chang, H.-Y. Lee, K. Chen, C.-C. Chang, D.-S. Tsai, C.-C. Fu, T.-S. Lim, Y.-K. Tzeng, C.-Y. Fang, C.-C. Han, H.-C. Chang, and W. Fann, "Mass production and dynamic imaging of fluorescent nanodiamonds," Nat. Nanotech. **3**, 284-288 (2008).
17. O. Faklaris, D. Garrot, V. Joshi, F. Druon, J.-P. Boudou, T. Sauvage, P. Georges, P. A. Curmi, and F. Treussart, "Detection of single photoluminescent diamond nanoparticles in cells and study of the internalization pathway," Small **4**, 2236-2239 (2008).
18. T.-L. Wee, Y.-W. Mau, C.-Y. Fang, H.-L. Hsu, C.-C. Han, and H.-C. Chang, "Preparation and characterization of green fluorescent nanodiamonds for biological applications," Diamond Relat. Mater. **18**, 567 (2009).
19. O. Faklaris, D. Garrot, V. Joshi, J.-P. Boudou, T. Sauvage, P. A. Curmi, and F. Treussart, "Comparison of the photoluminescence properties of semiconductor quantum dots and non-blinking diamond nanoparticles. Observation of the diffusion of diamond nanoparticles in living cells," J. Eur. Opt. Soc. Rapid Public. **4**, 09032 (2009).
20. V. Vaijayanthimala, Y.-K. Tzeng, H.-C. Chang, and C.-L. Li, "The biocompatibility of fluorescent nanodiamonds and their mechanism of cellular uptake," *Nanotech.* **20**, 425103 (2009).
21. T.-L. Wee, Y.-K. Tzeng, C.-C. Han, H. C. Chang, W. Fann, J. H. Hsu, K.-M. Chen, and Y.-C. Yu, "Two-photon excited fluorescence of nitrogen-vacancy centers in proton-irradiated type Ib diamond," J. Phys. Chem. A **111**, 9379-9386 (2007).
22. Y. Y. Hui, Y.-R. Chang, T.-S. Lim, H.-Y. Lee, W. Fann, and H.-C. Chang, "Quantifying the number of color centers in single fluorescent nanodiamonds by photon correlation spectroscopy and Monte Carlo simulation," Appl. Phys. Lett. **94**, 013104 (2009).
23. B**.** R. Smith, M. Niebert, T. Plakhotnik, and A. V. Zvyagin, **"**Transfection and imaging of diamond nanocrystals as scattering optical labels," J. Lumin. **127** 260–263 (2007).
24. L.-C. L. Huang and H.-C. Chang, "Adsorption and immobilization of cytochrome *c* on nanodiamonds," Langmuir **20**, 5879-5884 (2004).
25. N. Mohan, Y.-K. Tzeng, L. Yang, Y.-Y. Chen, Y. Y. Hui, C.-Y. Fang, and H.-C. Chang, "Sub-20-nm fluorescent nanodiamonds as photostable biolabels and fluorescence resonance energy transfer donors," Adv. Mater. **21,** 1-5 (2009). DOI: 10.1002/adma.200901596.
26. A. Krueger, Y. J. Liang, G. Jarre, and J. Stegk, "Surface functionalisation of detonation diamonds suitable for biological applications," J. Mater. Chem. **16**, 2322-2328 (2006).
27. C.-F. Chang, C.-Y. Chen, F.-H. Chang, S.-P. Tai, C.-Y. Chen, C.-H. Yu, Y.-B. Tseng, T.-H. Tsai, I.-S. Liu, W.-F. Su, and C.-K. Sun, "Cell tracking and detection of molecular expression in live cells using lipid-enclosed CdSe quantum dots as contrast agents for epi-third harmonic generation microscopy," Opt. Express **16**, 9534-9548 (2008).
28. Y. Dumeige, F. Treussart, R. Alleaume, T. Gacoin, J. Roch, and P. Grangier, "Photo-induced creation of nitrogen-related color centers in diamond nanocrystals under femtosecond illumination," J. Lumin. **109**, 61–67 (2004).
29. B. Dubertret, P. Skourides, D. J. Norris, V. Noireaux, A. H. Brivanlou, and A. Libchaber, "In vivo imaging of quantum dots encapsulated in phospholipid micelles," Sci. **298**, 1759-1762 (2002).
30. Y. Chen and Z. Rosenzweig, "Luminescent CdSe quantum dot doped stabilized micelles," Nano Lett. **2**, 1299-1302 (2002).
31. H. Fan, E. W. Leve, C. Scullin, J. Gabaldon, D. Tallant, T. Bunge, M. C. Wilson, and C. J. Brinker, "Surfactant-assisted synthesis of water-soluble and biocompatible semiconductor quantum dot micelles," Nano Lett. **5**, 645-648 (2005).
32. R. Bakalova, Z. Zhelev, I. Aoki, H. Ohba, Y. Imai, and I. Kanno, "Silica-shelled single quantum dot micelles as imaging probes with dual or multimodality," Anal. Chem. **78**, 5925-5932 (2006).
33. J. E. Schroeder, I. Shweky, H. Shmeeda, U. Banin, and A. Gabizon, "Folate-mediated tumor cell uptake of quantum dots entrapped in lipid nanoparticles," J. Control. Release **124**, 28-34 (2007).
34. N. Depalo, A. Mallardi, R. Comparelli, M. Striccoli, A. Agostiano, and M. L. Curri, "Luminescent nanocrystals in phospholipid micelles for bioconjugation: An optical and structural investigation," J. Colloid Interface Sci. **325**, 558-566 (2008).
35. M. J. Murcia, D. E. Minner, G. -M. Mustata, K. Ritchie, and C. A. Naumann, "Design of quantum dot-conjugated lipids for long-term, high-speed tracking experiments on cell surfaces," J. Am. Chem. Soc. **130**, 15054-15062 (2008).
36. A. Prakash, H. Zhu, C. J. Jones, D. N. Benoit, A. Z. Ellsworth, E. L. Bryant, and V. L. Colvin, "Bilayers as phase transfer agents for nanocrystals prepared in nonpolar solvents," ACS Nano **3**, 2139-2146 (2009).
37. V. P. Torchilin, "Recent advances with liposomes as pharmaceutical carriers," Nat. Rev. Drug Discov. **4**, 145-160 (2005).

#120224 - $15.00 USD Received 19 Nov 2009; revised 6 Jan 2010; accepted 7 Jan 2010; published 10 Mar 2010

38. P. Pallavicini, Y, A. Diaz-Fernandez, and L. Pasotti, "Micelles as nanosized containers for the self-assembly of multicomponent fluorescent sensors," Coord. Chem. Rev. **253**, 2226-2240 (2009).
39. A. M. Derfus, W. C. Chan, and S. N. Bhatia, "Probing the cytotoxicity of semiconductor quantum dots," Nano Lett. **4**, 11-18 (2003).
40. X. Gao, Y. Cui, R. M. Levenson, L. W. Chung, and S. Nie, "In vivo cancer targeting and imaging with semiconductor quantum dots," Nat. Biotechnol. **22**, 969-976 (2004).
41. A. M. Derfus, W. C. Chan, and S. N. Bhatia, "Intracellular delivery of quantum dots for live cell labeling and organelle tracking," Adv. Mater. **16**, 961-966 (2004).
42. V. Dudu, M. Ramcharan, M. L. Gilchrist, E. C. Holland, and M. Vazquez, "Liposome delivery of quantum dots to the cytosol of live cells," J. Nanosci. Nanotechnol. **8**, 2293-2300 (2008).
43. L. W. Zhang and N. A. Monteiro-Riviere, "Mechanisms of quantum dot nanoparticle cellular uptake," Toxicol. Sci. **110,** 138-155 (2009).
44. G. Gopalakrishnan, C. Danelon, P. Izewska, M. Prummer, P.-Y. Bolinger, I. Geissbühler, D. Demurtas, J. Dubochet, and H. Vogel, "Multifunctional lipid/quantum dot hybrid nanocontainers for controlled targeting of live cells," Angew Chem. Int. Ed. **45**, 5478-5483 (2006).

1. Introduction

Fluorescence correlation spectroscopy (FCS) and single particle tracking (SPT) are two commonly used techniques to study the dynamics of biomolecules and bioparticles in living cells [1-3]. Two-photon FCS [4-12] is an appealing technique because it has relatively low scattering background and probes fluorophores only in the vicinity of the laser focus. In two-photon excitation, the excited volume is small due to the quadratic dependence of the fluorescence intensity on light intensity, and thereby the photodamage to cells is significantly reduced. Additionally, the photoluminescence from the specimen can be observed without a confocal aperture and both the sensitivity and fluorescence image contrast are enhanced accordingly. Much work has been done in the past for two-photon FCS on nanometer-sized particles in solution [4-9]. However, reports on the two-photon FCS of nanoparticles (including fluorescent proteins) in cells are scarce [1, 2, 10-12]. Therefore, there is a need to further develop the techniques to facilitate our understanding of cellular dynamics.

Fluorescent nanodiamond (FND), containing nitrogen-vacancy defect centers in its crystal lattice, is an excellent candidate for use as fluorescent probes [13-19]. It is biocompatible and nontoxic [20], well suited for biomedical applications. Moreover, the material shows no sign of photobleaching, allowing for long-term monitoring in living cells. We have previously demonstrated that it is possible to observe single FND particles with a size in the range of 140 nm using an 875-nm femtosecond laser for two-photon excitation [16]. In that application, predominantly only the neutral nitrogen-vacancy (NV^0) centers were excited, as evidenced from the resulting fluorescence. The excitation, however, was not optimal for FNDs produced from type Ib diamond nanocrystallites, which often contain a larger quantity of negatively charged nitrogen-vacancy (NV^-) centers than NV^0 centers. Wee et al. [21] have determined that the NV^- center in diamond has a two-photon cross section of 0.45×10^{-50} cm^4s/photon at 1064 nm. The value is about 30-fold lower than that of rhodamine B. This deficit, fortunately, can be compensated for by using FNDs of 40 nm in diameter and containing more than 30 defect centers [22]. We demonstrate in this work that it is possible to detect these particles by two-photon excited luminescence with a femtosecond near-infrared laser (λ_{ex} = 1060 nm). In addition, two-photon FCS can be performed to probe the diffusion dynamics of FNDs in living cells.

Neugart et al. [15] has previously shown that FNDs coated with sodium dodecyl sulfate, a surfactant, can be internalized into HeLa cells after 3 h of incubation. However, most of the FND particles become immobile inside the cells after a short time. Freely diffusing single FND particles are rare. Faklaris et al. [19] have also investigated the diffusion of bare FNDs in HeLa cells, and determined a diffusion coefficient of < 0.01 $\mu m^2/s$. In a separate work, Smith et al. [23] applied non-fluorescent nanodiamond particles to a lipid-rich serum-free medium and cationic liposomes. The resultant lipid-coated nanodiamond particles were effectively transfected into mammalian cells, but the diffusion coefficient of these particles in the cells was not reported. Herein, we demonstrate that the encapsulation of FNDs within

#120224 - $15.00 USD Received 19 Nov 2009; revised 6 Jan 2010; accepted 7 Jan 2010; published 10 Mar 2010

cationic cholesterol-based lipids makes the particles become mobile in the cytoplasm of the cells. The diffusion coefficient markedly increases by more than one order of magnitude.

2. Experimental section

FNDs (~40 nm in diameter) were prepared by 40-keV He^+ ion beam irradiation and vacuum annealing at 800 ºC, followed by air oxidation and strong oxidative acid treatments [24, 25]. Before loading of FNDs, HeLa cells (10^5 cells per mL) were first cultured in Dulbecco's modified Eagle's medium (DMEM, HyClone, SH30243.02) supplemented with 10% fetal bovine serum and 1% penicillin/streptomycin in a chamber slide. Suspensions of the FNDs were then diluted with DMEM without serum to a final concentration of 1 μg/ml and added to the medium. The cells were incubated at 37 °C in a 5% CO_2 incubator for 5 h, after which they were observed by a modified confocal fluorescence microscope for both one-photon and two-photon excited luminescence measurements.

In the one-photon experiment, the FND particles either suspended in water, spin-coated on glass slides, or internalized by cells were excited by a solid state laser (JL-LD532-GTE, Jetlaser) operated at 532 nm with an excitation power of 0.2 mW [14]. The laser was focused to a diffraction-limited spot by an oil immersion objective (Nikon E600, 100×, NA 1.3). The resulting fluorescence, after passing through two filters (555LP and 750SP, Chroma), was collected by an avalanche photodiode (Perkin Elmer). Fluctuations of the fluorescence were recorded with a time-correlated single photon counting module (PicoHarp 300, PicoQuant) and analyzed by the SymPhoTime Software for correlation analysis. The structure parameter and the radius of the confocal volume required in the FCS measurements were determined independently from the free diffusion of rhodamine 6G and FluoSpheres fluorescent microspheres (F8786 and F8801, Molecular Probes) in water [25].

In the two-photon experiment, we directed a femtosecond Nd:glass laser (IC-1060-100, High Q laser) to the same confocal fluorescence microscope. The laser (λ = 1060 nm) has a pulse width of 180 fs, an average output power of >100 mW, and a repetition rate of 72 MHz. The typical power of the laser after passing through the oil immersion objective was 10 mW, which is close to the photodamage threshold (~15 mW) of the cells.

In a separate experiment, we tracked the movement of FNDs in HeLa cells by one-photon excitation using a three-dimensional SPT system as previously described [16]. The system consisted of a wide-field microscope equipped with an electron-multiplier CCD camera (DV887DCS-BV, Andor), and a microscope objective (Plan-Apo 100×, NA 1.4; Olympus) mounted vertically on a *z*-motion piezoelectric translational stage (MCLS F100, Mad City Labs). In this experiment, the HeLa cells typically lived for more than 2 h, which was comparatively longer than our observation duration in few minutes. We have also attempted to collect a two-photon-excited wide-field fluorescence images using the same setup. However, the power density was not high enough for two-photon excitation. Also, the illuminated area on the sample was restricted by few μm^2, which is too small for SPT. Further increase of the infrared laser power led to photodamage to the cells.

For lipid coating, FNDs were first hydroxylated [26] by adding dry powders (20 mg) to 1 M BH_3 in tetrahydrofuran (8 ml) under nitrogen atmosphere and sonicated until the FND particles were well suspended in the solution. The mixture was then stirred under reflux for 24 h, followed by addition of 1 N HCl to stop the reaction. After separation of the mixture by centrifugation at 15,000 rpm for 15 min, the supernatant was removed and the residue was thoroughly washed with acetone and finally dried with nitrogen. The resulting hydroxylated FNDs were silanized by adding the particles to a solution containing toluene (8 ml) and octadecyltrimethoxysilane (0.15 ml) and fully dispersed by sonication. The mixture was stirred at room temperature for 24 h, after which the hydrophobized FNDs were separated by centrifugation and washed thoroughly with acetone and water and dried with nitrogen. Finally, the dried hydrophobized FNDs and lipids were mixed in chloroform, desiccated by evaporation of chloroform, and resuspended in 5% dextrose solution by sonication to form lipid-encapsulated FNDs [27]. To improve the particle solubility and cellular uptake, 3-β-[N-(2-guanidinoethyl)carbamoyl]-cholesterol (GEC-Chol) and cholesterol (in a 1:1 molar ratio)

#120224 - $15.00 USD Received 19 Nov 2009; revised 6 Jan 2010; accepted 7 Jan 2010; published 10 Mar 2010

were used as the lipid ingredients in the formulation of cationic lipid-encapsulated FNDs. Due to the lipid coating, the diameter of the 40-nm FNDs increased to 150 nm as determined from dynamics light scattering measurements. The sizes of the particles before and after the lipid coating were further determined by one-photon and two-photon FCS in water. These results are shown in Table 1.

Table 1. Diffusion coefficients and particle sizes of bare and lipid-encapsulated FNDs determined by one-photon and two-photon FCS in water

	Diffusion coefficient (Particle size)	
	One-photon FCS	Two-photon FCS
Bare FND	8.8 $\mu m^2/s$ (45 nm)	9.6 $\mu m^2/s$ (50 nm)
Lipid-encapsulated FND	2.6 $\mu m^2/s$ (160 nm)	2.8 $\mu m^2/s$ (170 nm)

3. Results and discussion

We firstly recorded the confocal scanning two-photon fluorescence images of bare 40-nm FNDs spin-coated on glass plates, and compared them with corresponding one-photon images. These bare FND particles were prepared with air oxidation and strong oxidative acid treatments and, therefore, their surfaces are decorated with a variety of oxygen-containing groups [24]. Figure 1a shows diffraction-limited images of the individual particles in these two excitation cases, demonstrating single particle detection capabilities of both techniques. Applying the same techniques to detect single FNDs in HeLa cells reveals that the image contrast due to the two-photon excitation is significantly enhanced, primarily due to reduction of the cell autofluorescence in the excitation region (Fig. 1b). The intensity ratio between the FND fluorescence and the cell autofluorescence in the two-photon excitation is at least 2 times better than that in the one-photon excitation. Figure 2 shows the corresponding fluorescence spectra of the particles dispersed on glass plates. In contrast to the two-photon excited luminescence obtained with the 875 nm femtosecond laser [16, 28], where predominantly only the spectral features of NV^0 centers were observed, the characteristic signatures of the NV^- center can be found in the spectrum when the near-infrared excitation (λ_{ex} = 1060 nm) was used as the light source. Excitation at higher laser powers (~15 mW), however, irreversibly converted some of the NV^- centers to NV^0 [28].

#120224 - $15.00 USD Received 19 Nov 2009; revised 6 Jan 2010; accepted 7 Jan 2010; published 10 Mar 2010

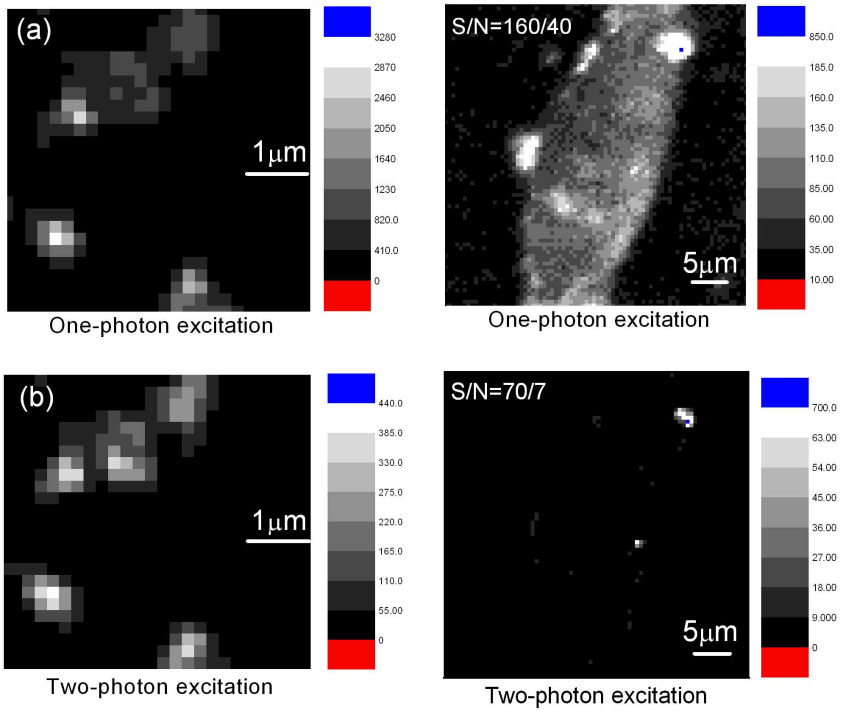

Fig. 1. (a) One-photon and (b) two-photon excited luminescence images of 40-nm FNDs on glass slides (left) and in HeLa cells (right). The power of the green laser used to excite FND particles in HeLa cells (or on glass slides) is 70 μW (or 700 μW), while the infrared laser power is 5 mW (or 10 mW). The unit of the fluorescence intensity is 100 counts per second.

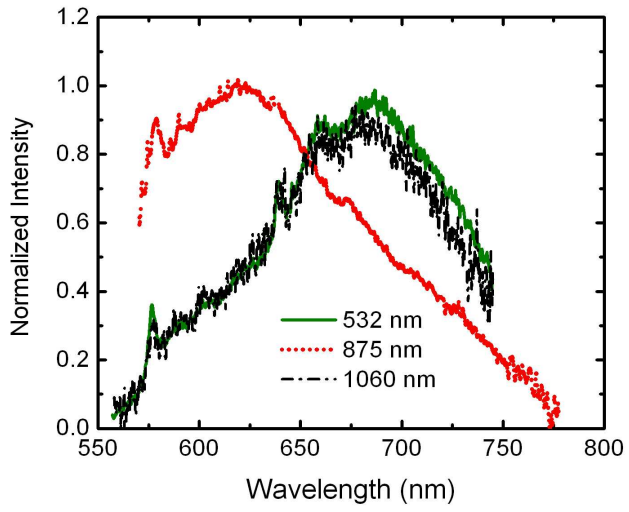

Fig. 2. Comparison of one-photon and two-photon excited luminescence spectra of bare 40-nm FNDs with 532, 875, and 1060 nm lasers.

#120224 - $15.00 USD Received 19 Nov 2009; revised 6 Jan 2010; accepted 7 Jan 2010; published 10 Mar 2010

We exploit the advantage of the two-photon excitation to investigate the FND movement in living cells by FCS. As previously found, most FNDs after purification in strong oxidative acids are immobile in the HeLa cell [16, 19]. As a result, there is no time-intensity correlation signal from the acid-treated FNDs in the cell, since most of them (~90%) do not move in the cytoplasm within the typical detection time of 60 s to even 5 min (Fig. 3). This negative result is in good agreement with previous reports that FND particles can undergo autonomous cellular internalization [13] but are immediately trapped during endocytosis [14-17]. To overcome this problem, we coated FNDs with lipids, forming liposome- or micelle-like particles [29-36].

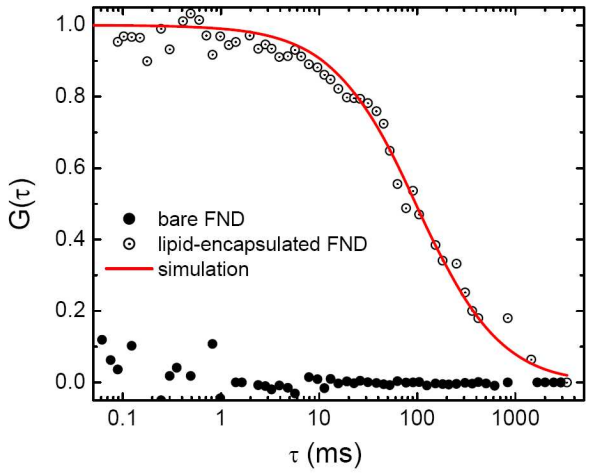

Fig. 3. Two-photon FCS of bare and lipid-encapsulated 40-nm FNDs in live HeLa cells. The solid line is the fit of experimental data using Eq. (1).

Liposomes and micelles represent two prototypic nanoparticle systems that have been fully optimized for in vivo human use as drug carriers [37, 38]. The lipid coating, in particular, has been applied to encapsulate quantum dots to minimize the cytotoxicity of the material [39]. Also, the aggregation of nanoparticles in cells and in vivo can be prevented by the lipid encapsulation [40, 41].

We coated FNDs with lipids following the procedures illustrated in Fig. 4a [26]. As shown in the photo of Fig. 4b, the FNDs become highly hydrophobic after the reduction and silanization treatments, and all the particles prefer to stay in the organic phase (toluene in this case). These hydrophobic particles can then be encapsulated by lipids, forming liposomes as detailed in the experimental section. Figure 4c compares the fluorescence spectra of the bare and lipid-encapsulated FNDs. These two spectra are very similar to each other except that some fluorescence background arising from excitation of the lipids appears at near 600 nm. Overall, the lipid coating does not affect the spectra, which is not too surprising as the NV color center lies deep under the nanodiamonds. The chemical environment does not influence the emission properties of the NV centers, which is a distinct advantage of using FNDs over quantum dots for biolabeling applications [14].

#120224 - $15.00 USD Received 19 Nov 2009; revised 6 Jan 2010; accepted 7 Jan 2010; published 10 Mar 2010

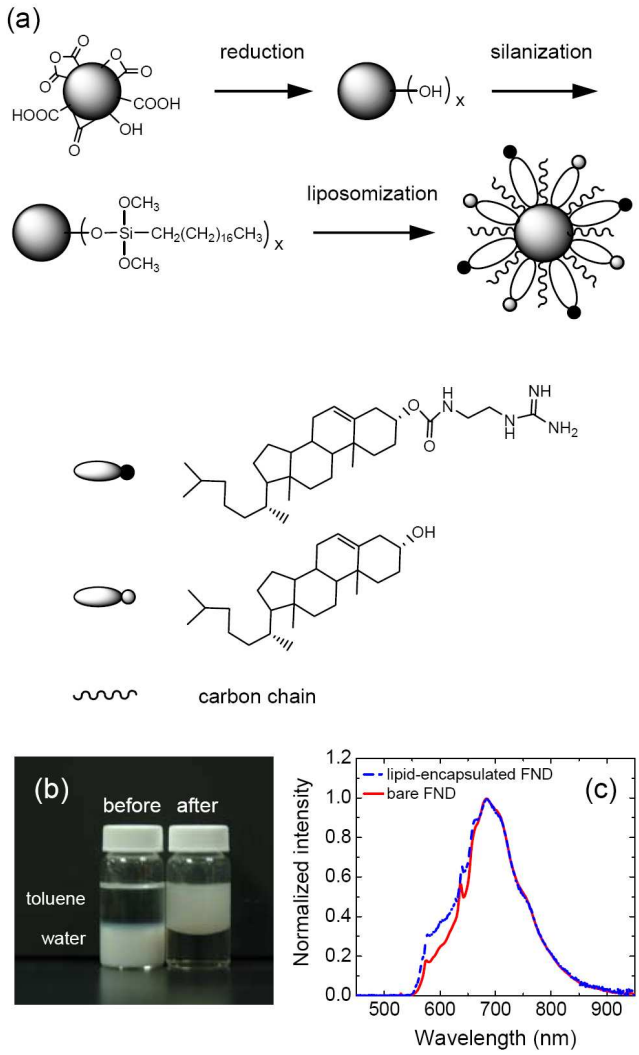

Fig. 4. (a) Synthesis of lipid-encapsulated FNDs by reduction, silanization, and liposomization (lipid encapsulation) reactions. (b) Photograph of 40-nm FNDs suspended in toluene/water before and after the reduction and silanization treatments described in text. (c) Fluorescence spectra of bare and lipid-encapsulated 40-nm FNDs suspended in water.

The lipid-encapsulated FNDs were loaded into HeLa cells by incubation of the particles with the cells in DMEM for 3 h, followed by observation with the one-photon excited luminescence SPT system. Roughly 1 out of 10 lipid-encapsulated nanodiamonds was found to diffuse freely in the cells. We checked the FND movement and analyzed the two-photon fluorescence intensity fluctuation. A typical correlation curve of the internalized lipid-encapsulated FNDs is shown in Fig. 3. In marked contrast to the stationary motion of the bare FNDs, the movement of the lipid-encapsulated particles becomes now visible. We analyzed the intensity fluctuation and fitted it to the autocorrelation function [2],

$$G(\tau) = \frac{1}{1+\frac{\tau}{\tau_D}} \bullet \frac{1}{\sqrt{1+\frac{\tau}{s^2\tau_D}}} \qquad (1)$$

#120224 - $15.00 USD Received 19 Nov 2009; revised 6 Jan 2010; accepted 7 Jan 2010; published 10 Mar 2010

where τ_D is the average residue time in the focal volume if there is only diffusion, and s is the structure parameter determined by calibration against fluorescent nanospheres of known sizes. Meanwhile, the diffusion coefficient is given by $D = r_0^2/8\tau_D$ for two-photon FCS [2], where r_0 is the radius of the confocal volume. We found that the diffusion coefficient of the lipid-encapsulated FNDs in the HeLa cell is 0.08±0.04 $\mu m^2/s$, which represents an enhancement by a factor of >10 over that of the bare FNDs (Table 1).

While FCS is a powerful means in exploring the dynamics of fluorescent particles in solution and cells, it probes only fluorophores in the vicinity of the excited region. The technique is not suitable for dynamic tracking of the same particle over a long period of time and its movement in three dimensions. SPT offers the alternative [3]. With one-photon excited luminescence, we monitored the targeted FND in the HeLa cell by SPT and recorded its three-dimensional trajectory under a wide-field fluorescence microscope. Though the bare FNDs rarely move in the cell, we found few exceptional cases in our observations [16]. A typical trajectory of the FND is displayed in Fig. 5, from where the corresponding mean square displacement (MSD) is computed. We approximate the motion by $MSD = 6Dt + (vt)^2$, where v is the transport velocity of the particle [3], and determine a diffusion coefficient of $D = 3 \times 10^{-3}$ $\mu m^2/s$. The value, clearly, is too small to be detected in the FCS measurement (Fig. 3). We have also measured the diffusion coefficient of the lipid-encapsulated FND in the same cancer cell. As evidenced from the slopes of the trajectories shown in Fig. 5, the lipid encapsulation around the FND improves the diffusion coefficient of the particle by nearly one order of magnitude. The enhanced diffusion, confirmed in both FCS and SPT measurements, indicates that the lipid-encapsulated FNDs, most likely, enter the cells via a non-endocytosis pathway. In this pathway, lipid-mediated fusion of the particle with the cell membrane occurs [42, 43].

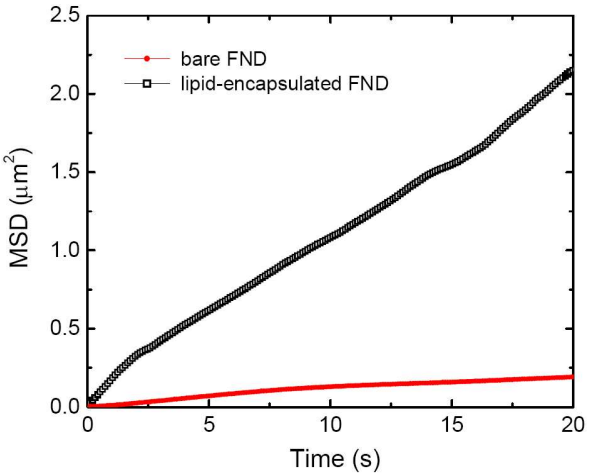

Fig. 5. Single-particle tracking of FNDs in HeLa cells using one-photon excited luminescence in the cases of bare and lipid-encapsulated 40 nm particles.

Finally, we compare in Table 2 the diffusion coefficient of our FNDs in cells with that of lipid-coated quantum dots on cell surfaces [35, 44]. The large difference in diffusion coefficient between them can be properly accounted for by their differences in size as well as in cellular environment. In our future experiments, we will encapsulate sub-20 nm FNDs [25] in various types of lipids so that faster cellular dynamics, similar to that of quantum dots, can be probed and analyzed either in cells or on cell surfaces at the single particle level.

#120224 - $15.00 USD Received 19 Nov 2009; revised 6 Jan 2010; accepted 7 Jan 2010; published 10 Mar 2010

Table 2. Comparison of diffusion coefficients of lipid-coated nanoparticles in cells and on cell surfaces, determined by FCS

Nanoparticles	Sizes (nm)	Lipids	Diffusion coefficients ($\mu m^2/s$)	References
FND	150	GEC-Chol[a]	0.08	This work
CdSe/ZnS	33	DHPTE[b]	0.63[d]	[35]
CdSe	60[e]	DMPC[c]	0.3[d]	[44]

[a]3-β-[N-(2-guanidinoethyl)carbamoyl]-cholesterol (GEC-Chol), [b]1,2-dipalmitoyl-*sn*-glycero-3-phosphothioethanol (DHPTE), [c]1,2-Dimyristoyl-sn-glycero-3-phosphatidylcholine (DMPC), [d]On cell surfaces, [e]Average value

To conclude, we have demonstrated that the image contrast of FNDs in living cells can be enhanced by two-photon excitation. In addition, the lipid encapsulation around FNDs improves the diffusion coefficients of the particles in the cytoplasm of the cells by more than an order of magnitude. The combination of two-photon FCS with one-photon SPT has allowed both short-term and long-term tracking of single FNDs in complex biological environment.

Acknowledgements

This work is supported by the National Science Council, Taiwan with Grant No. NSC 97-2120-M-001-005 and NSC 97-2112-M-110-008-MY2.

#120224 - $15.00 USD Received 19 Nov 2009; revised 6 Jan 2010; accepted 7 Jan 2010; published 10 Mar 2010